Characteristics of Irradiated Silicon Microstrip Detectors with $\langle 100 \rangle$ and $\langle 111 \rangle$ Substrates

T. Akimoto [a] S. Arai [a] K. Hara [a] T. Nakayama [a] Y. Ikegami [b] Y. Iwata [c] T. Kohriki [b] T. Kondo [b] I. Nakano [d] T. Ohsugi [c] M. Shimojima [a] S. Shinma [a] R. Takashima [e] S. Terada [b] N. Ujiie [b] Y. Unno [b] K. Yamamoto [f] K. Yamamura [f]

[a] *University of Tsukuba, Institute of Physics, Tsukuba, Ibaraki 305-8571, Japan*

[b] *IPNS, High Energy Accelerator Organization (KEK), Tsukuba, Ibaraki 305-0801, Japan*

[c] *Hiroshima University, Dep. of Physics, Higashi-Hiroshima, Hiroshima 739-8526, Japan*

[d] *Okayama University, Dep. of Physics, Okayama, Okayama 700-8530, Japan*

[e] *Kyoto University of Education, Dep. of Education Fushimi, Kyoto 612-0863, Japan*

[f] *Solid State Division, Hamamatsu Photonics K.K., Hamamatsu, Shizuoka 435-8558, Japan*

Abstract

In a program of developing radiation-hard silicon sensors for the LHC-ATLAS experiment, we have irradiated various types of silicon sensors with 12-GeV protons at KEK, and made a comparative study, among the other properties, of characteristics of the sensors with two wafer planes $\langle 111 \rangle$ and $\langle 100 \rangle$. The studied sensors are p-on-n type, which satisfy the ATLAS-SCT specifications. Possible dependence on the substrate orientation could result from different dangling-bond configurations. The compared characteristics are the charge collection efficiency, interstrip capacitance, and noise levels measured with a real ATLAS-SCT electronics system. A substantial difference is observed in the interstrip capacitance at $\sim$10 kHz, while the difference is small at $>$1 MHz. Also the differences in the charge collection efficiency and in the noise levels appear to be small.

Key words: silicon microstrip detector; radiation damage; wafer direction; $\langle 111 \rangle$; $\langle 100 \rangle$; charge collection; interstrip capacitance; ATLAS SCT;

1 Introduction

Silicon microstrip detectors will be extensively used for tracking in the ATLAS experiment at the LHC. The ATLAS SCT (Semiconductor Tracker) system is described in detail in [1]. The sensors are AC-coupled and single sided with dimensions of 63.56 (width) $\times$ 63.96 (length) $\times$ 0.28 (thickness) mm^3. The electrode strips of 12 μm width are made on the p side at a pitch of 80 μm with the number of readout strips being 768. Two fo such sensors are wire-bonded together, constructing a readout strip length of $\sim$12 cm. The radiation tolerance is one of the key issues to operate silicon microstrip detectors in ATLAS, where the radiation environment is estimated to correspond to 3 $\times 10^{14}$ multi-GeV proton equivalent per cm^2 in 10 years of operation.

In a program of developing radiation-hard silicon sensors, we have fabricated various types of silicon sensors and irradiated them with 12-GeV protons at KEK. The irradiations were performed for two separate sets of sensors to 1.7×10^{14} cm^{-2} and 4.2×10^{14} cm^{-2}. The present measurements were made 6–12 months after the initial annealing is completed. The details of the irradiation conditions and performance tests which include the leakage current increase, change in the full depletion voltage and drop in the charge collection are reported elsewhere[2].

In this report, we examine the possible difference between the sensors with the two wafer planes, $\langle 100 \rangle$ and $\langle 111 \rangle$. The compared sensors are summarized in Table 1. All the sensors are the p-on-n type, satisfying the ALTAS-SCT specifications. Comparative studies are made on the charge collection efficiency, interstrip capacitance, and noise performance. As pointed out in [3], different behaviors between these wafer orientations could result from the different amount of the dangling bonds at the Si-SiO_2 interface.

Table 1
Tested silicon microstrip sensors. * is either 0, 17 or 42, denoting the proton fluence in unit of 10^{13} cm^{-2}.

sensor name	maker	resistivity	wafer plane	fluence (cm^{-2})
Hp4k-*	Hamamatsu	4 kΩcm	$\langle 111 \rangle$	0, 17 $\times 10^{13}$
Hp1k-*	Hamamatsu	1 kΩcm	$\langle 100 \rangle$	17, 42 $\times 10^{13}$
Sp4k-*	SINTEF	4 kΩcm	$\langle 100 \rangle$	17, 42 $\times 10^{13}$

2 Charge collection

The charge collection could degrade due to trapping and recombination centers created by intense radiation. The surface charge accumulation could also modify the electric field around the strips and hence the charge collection efficiency. If the influence associated with the wafer orientation emerges itself only at the Si-SiO_2 interface and not in the bulk, we expect small difference at least in the former effect.

The charge collection curves were measured using penetrating β rays from a ^{90}Sr source[2]. The sample sensor was sandwiched between a pair of Aℓ slits with a scintillation counter set underneath, which created gate signals to an ADC. Three adjacent strips were read out separately. The peak ADC count of the summed signals is plotted as a function of the bias voltage. Figure 1 is an excerption from [2], which shows the charge collection curves of the three types of the sensors irradiated to 1.7×10^{14} cm^{-2}. The ordinate is normalized by the charge collection plateau of a non-irradiated Hp4k sample.

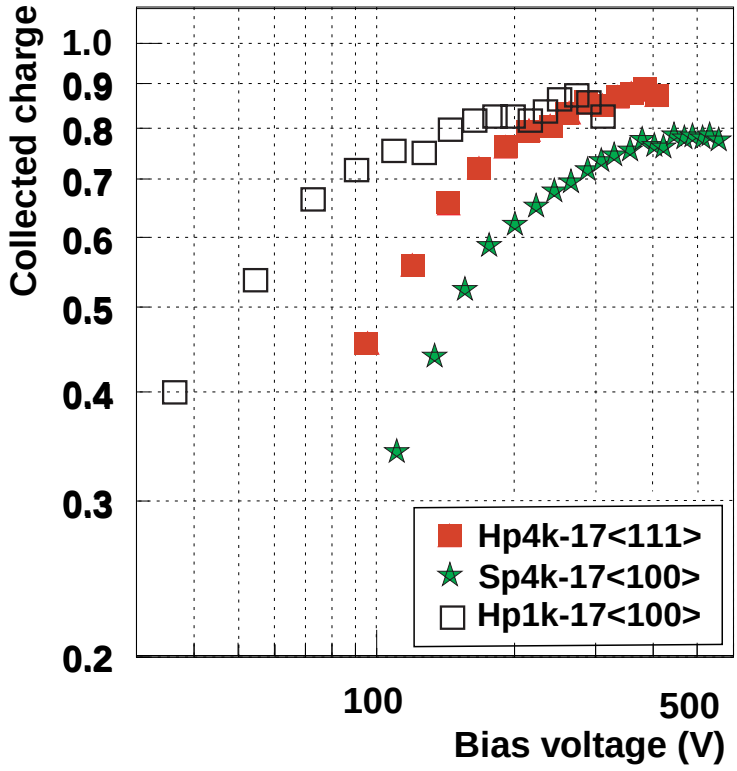

Fig. 1. Charge collection curves of the three sensors irradiated to 1.7×10^{14} protons cm^{-2}. The vertical axis is normalized by the charge collection plateau of an Hp4k-0 sensor.

We note that the shapes of Hp4k-17 and Sp4k-17 sensors are similar whereas the Hp1k-17 curve remains high at lower voltages, which is due to the difference in the initial resistivity.

In Fig. 2 we plot the charge collection values at plateau for various samples we tested. Typically there are measurements for two samples at the same condition (only one for SINTEF), which are plotted by the same marks in the figure. Although the set of the samples is not complete, there seems small difference between $\langle 111 \rangle$ and $\langle 100 \rangle$ wafer orientations. As is pointed out in [2], though, n-on-n sensors are superior to p-on-n sensors in the charge collection, since the junction side of irradiated n-on-n sensors is on the strip side and the electric field becomes preferable for charge collection.

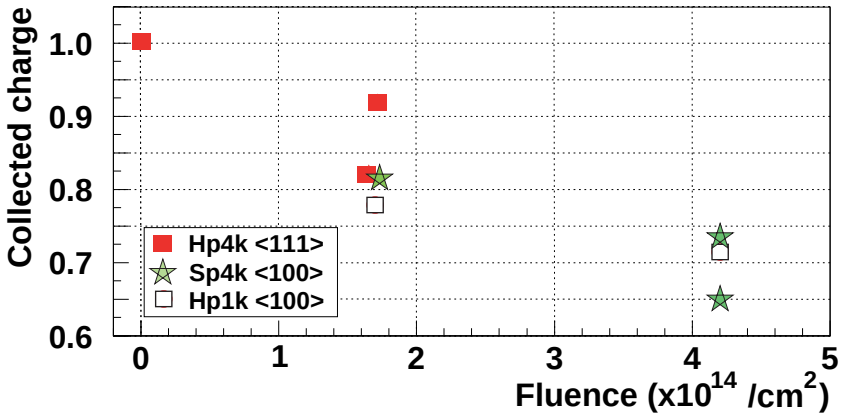

Fig. 2. The charge collection of three types of the sensors as a function of proton fluence.

3 Interstrip capacitance

The characterization of the interstrip capacitance was based on an HP4192A LCR meter. Several Aℓ strips were wire-bonded to a printed circuit board, which provided the connection to the LCR meter through Lemo cables. Hereafter we define the interstrip capacitance as that between two neighboring strips with the adjacent strips floating.

Figure 3 shows the frequency dependence of the interstrip capacitance. The bias voltages were set on the plateau in the charge collection curves. Non-irradiated sample exhibits a cutoff at a few kHz, which is due to existence of bias resistors parallel to the interstrip capacitance. The irradiated Hp1k $\langle 100 \rangle$ sensors show a small deviation at a frequency lower than 10 kHz. The curves of Sp4k-17 and Sp4k-42 (not shown in the plot, which behaves similar to Sp4k-17) show a larger deviation than Hp1k sensors. However, these curves are essentially similar in the shape, considering the cutoff of SINTEF sensors being at a smaller frequency. On the contrary, the irradiated $\langle 111 \rangle$ sensors show an enhancement of $\sim$30% in a wider frequency range below $\sim$100 kHz. They all, however, tend to become identical above $\sim$5 MHz. It can be concluded that the frequency dependence of the interstrip capacitance is not dependent

on the proton fluence in the range we investigated. Since a major difference in the curves is observed between ⟨100⟩ and ⟨111⟩ sensors, the wafer orientation should be attributed to the changes.

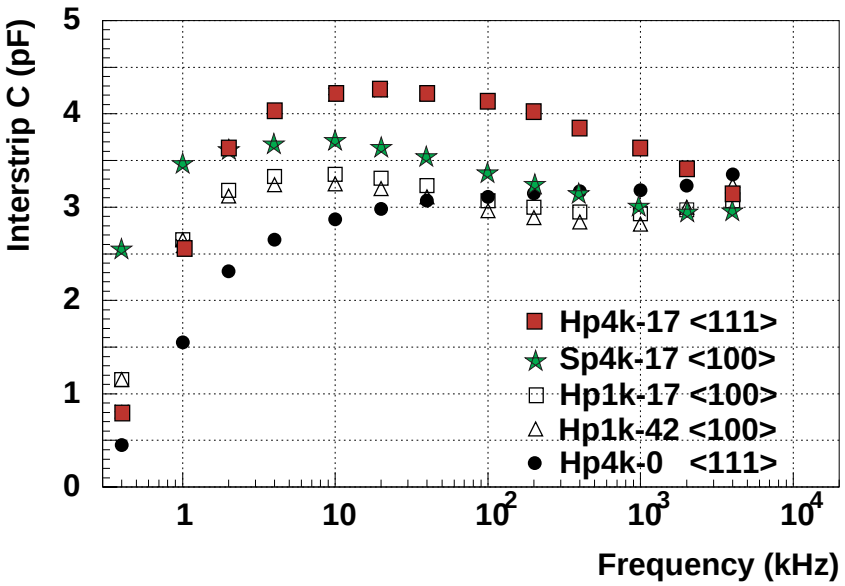

Fig. 3. Frequency dependence of the capacitance between neighboring strips. The bias voltage is set on the plateau in the charge collection curves.

We evaluated the bias voltage dependence of the interstrip capacitance at 10 kHz, where the difference appears to be most distinctive. The results are shown in Fig. 4. While the interstrip capacitance at lower bias voltages seems different between Hp1k-17 and Sp4k-17 sensors, it converges into a similar value at the full depletion voltage of ∼300 V. The different behavior at lower voltages should be related to the difference in the wafer resistivity. On the other hand, the interstrip capacitance of Hp4k-17 is high at lower voltages and continues to decrease across the full depletion voltage, resulting that the interstrip capacitance is higher than the others even at 300 V.

It is reported in [3] that the interstrip capacitance is influenced more by irradiation if the frequency is decreased (from 1 MHz to 100 kHz) and the bias voltage is lowered (from 500 V to 300 V) for ⟨111⟩ substrate with resistivity of 6 kΩcm. It also reports that there is essentially small change for ⟨100⟩ substrate with resistivity of 1 kΩcm. The present results are qualitatively consistent with their measurements.

4 Contribution to the electronics noise

The interstrip capacitance contributes dominantly to the detector capacitance. The actual contribution to the electronics noise may not be substantial since

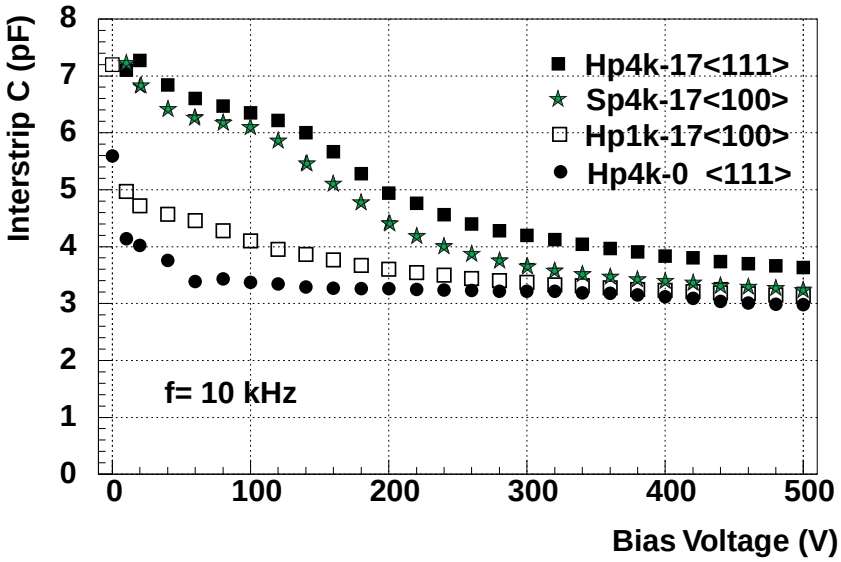

Fig. 4. Interstrip capacitance at 10 kHz as a function of bias voltage.

the increase is small in the range above 1 MHz which is the responsible frequency range for the electronics.

The contribution to the electronics noise was evaluated by using a non-irradiated real SCT readout system based on ABCD2T front-end chips. One ABCD2T chip (128 readout channels) was mounted on a flexible Kapton-based hybrid. Consecutive 6-cm long 16 strips were wire-bonded to the ABCD2T chip through a pitch adapter. Another consecutive 16 strips were also wire-bonded to the same chip inputs, thereby simulating 12 cm long strips in the real SCT configuration. The sample was placed in a thermostat chamber with the temperature being kept at -10°C. The same input channels of the same ABCD2T chip are used in order to compare the noise levels of the different sensor types.

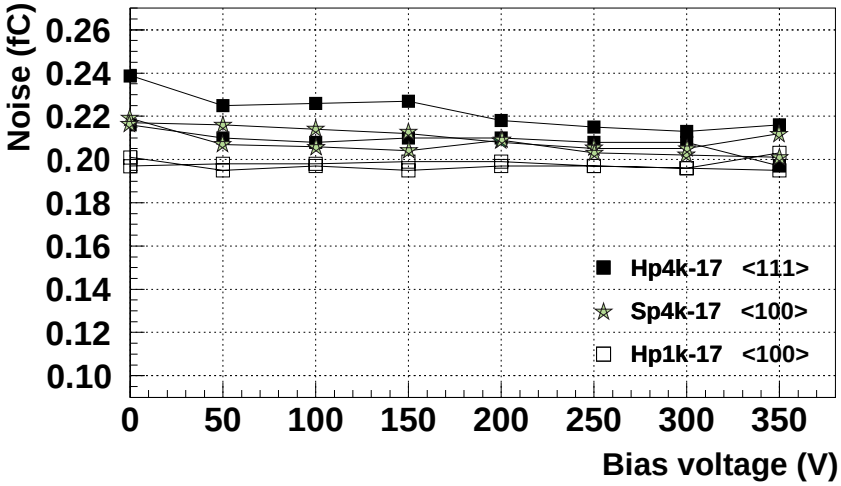

Fig. 5. Noise as a function of the bias voltage for the three types of irradiated sensors, two sensors for each.

The ABCD2T is a binary readout system, therefore the noise was evaluated from the sigma of the error function which was fitted to the efficiency vs injected charge relation at a given comparator threshold voltage. The threshold voltage was adjusted to correspond to 2 fC of the charge injection. The noise values of the connected 16 channels are consistent to each other. We plot in Fig. 5 the noise average of the central channels only, though, in order to avoid the possible influence from the unconnected strips. Two sensors were measured for each of the three types irradiated to 1.7×10^{14} cm^{-2}. Although the noise levels at 300 V, where all the sensors are on the full depletion plateau, show that Hp4k-17 ($\langle 111 \rangle$) tends to be somewhat larger than Hp1k-17 and Sp4k-17 ($\langle 100 \rangle$) by 5–7%, the significance is weak due to the systematic uncertainty of $\sim$3%. Note that the noise level for a non-irradiated sensor is 0.20 fC.

In the figure we show the noise levels up to 350 V. Above this voltage the noise level was found to increase. The sensors we used in this study are based on "1997 design" where a substantial micro-discharge is observed around the guard rings. The current design ("1998 design") has modified the layout and such an increase is not observed [5].

5 Summary

We have evaluated the characteristics of silicon microstrip sensors irradiated with protons and compared the results in view of $\langle 111 \rangle$ and $\langle 100 \rangle$ substrate orientations. The comparison was performed on the charge collection, interstrip capacitance, and the contribution to the electronics noise. Although an increase of 30% was observed for $\langle 111 \rangle$ in the interstrip capacitance at $\sim$10 kHz, there are small differences in other characterstics. The noise levels measured with a real SCT electronics system agreed to each other to a level of 5–7%.

References

[1] ATLAS Technical Design Report 5, CERN/LHCC/97-17 (1997).

[2] T. Nakayama et al., "Radiation damage studies of silicon microstrip sensors", Proceedings for 1999 IEEE Nuclear Science Symposium, 24-30 October 1999, Seattle, WA, USA.

[3] S. Albergo et al., "Comparative study of 111 and 100 crystals and capacitance measurements on Si strip detectors in CMS", Nuovo Cimento A, 112A (1999) 1261.

[4] W. Dabrowski et al., "The ABCD Binary Readout Chip for Silicon Strip Detectors in the Atlas Silicon Tracker", Proc. of the Fourth Workshop

on Electronics for LHC Experiments, Rome, Spetember 21-25, 1998, CERN/LHCC/98-36, p.175. Updates to the current version ABCD3T can be found in:
http://scipp.ucsc.edu/groups/atlas/elect-doc/ABCD3T_Spec_v1.1.pdf.

[5] D. Morgan et al., "Chanracterization of p-in-n silicon microstrip detectors fabricated by Hamamatsu Photonics and irradiated with 24-GeV/c protons to 3 $\times 10^{14}$ p/cm^{-2}, Nuovo Cimento A, 112A (1999) 1245.